Journal of Zhejiang University-SCIENCE A (Applied Physics & Engineering)

Design methodology of an osculating cone waverider with adjustable sweep and dihedral angles
(后掠角及反角可控的吻切锥乘波体设计方法)

Shao-hua CHEN

Cite this as: Shao-hua Chen, Jun Liu, Wei Huang, Feng Ding, 2020. Design methodology of an osculating cone waverider with adjustable sweep and dihedral angles. *Journal of Zhejiang University-SCIENCE A (Applied Physics & Engineering)*, 21(9):770-782. https://doi.org/10.1631/jzus.A2000020

研究目的

- Key design parameters concerned with lateral stability and lift-to-drag ratio introduced to the waverider design process: the dihedral angle, the sweep angle
- The influence evaluations of dihedral and sweep angle on the lateral stability and lift-to-drag ratio of waverider.

JZUSA

创新要点

1、Another way to reach osculating cone waverider based on planform leading edge profile curve

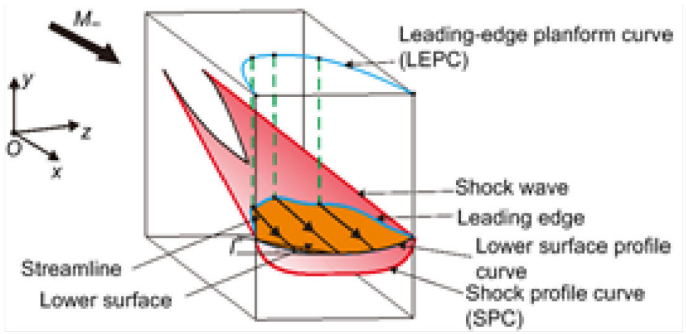


Fig. 2 Osculating cone waverider design method defined by the leading-edge planform profile

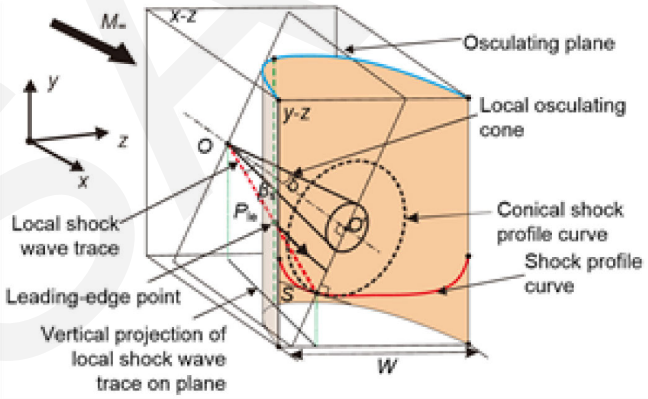


Fig. 4. 3D geometrical relationships for locating the leading-edge point on each osculating plane

This study uses the osculating cone waverider design method defined by the leading-edge planform profile, as illustrated in Fig. 2. The leading-edge planform curve is used to find the leading edge. The 3D leading edge in the shock wave is the vertical projection of the leading-edge planform curve. As shown in Fig. 4, a streamline starting from the leading-edge point is solved in the osculating plane. The leading-edge point P_{le} is also the intersection point of the local shock wave trace and the leading-edge planform curve (LEPC) on each osculating plane. The coordinate of point S in the shock profile curve is given in the osculating cone waverider method. The coordinate of point O, known as the cone vertex, depends on the geo-metrical relationships shown in Fig. 4.

创新要点

2、Design methodology of osculating cone waverider with adjustable sweep and dihedral angles

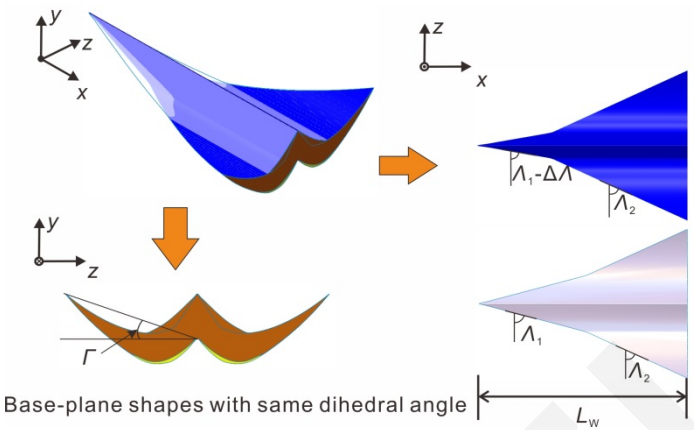


Fig. 6 Waveriders with different sweep angles (Λ) and the same dihedral angle (Γ)

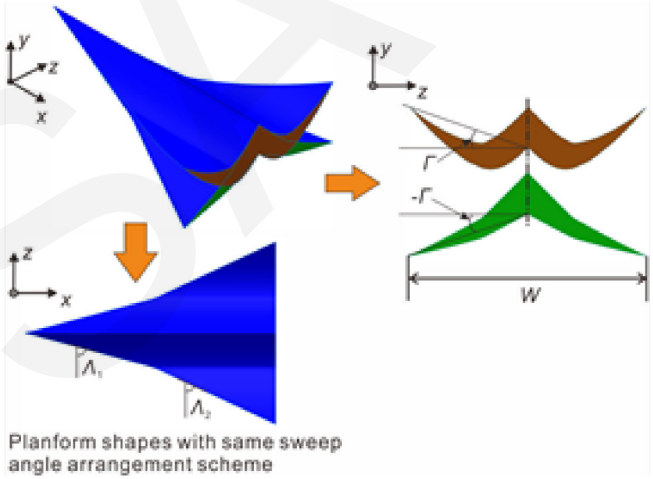


Fig. 7 Waveriders with different dihedral angles (Γ) and the same sweep angle (Λ)

As shown in Figs. 6 and 7, the geometries of design examples with different sweep angles or dihedral angles are generated. As presented in Fig. 6, two different sweep angle combination schemes are used in different waveriders with given length and width. As Fig. 6 denotes, the two waveriders have the same dihedral angle. Furthermore, the dihedral angle can be adjusted without changing the sweep angle. As depicted in Fig. 7, positive and negative dihedral angles are respectively assigned to two different waveriders. Meanwhile, they have the same planform contour and the same sweep angle distribution along the spanwise direction.

创新要点

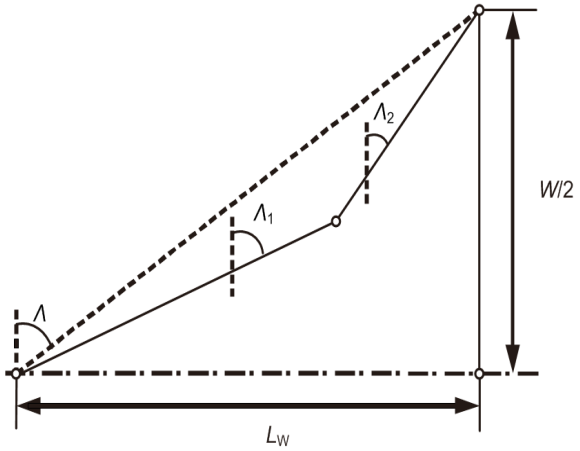


Fig. 8 Waverider planform geometric characteristics curves (right half)

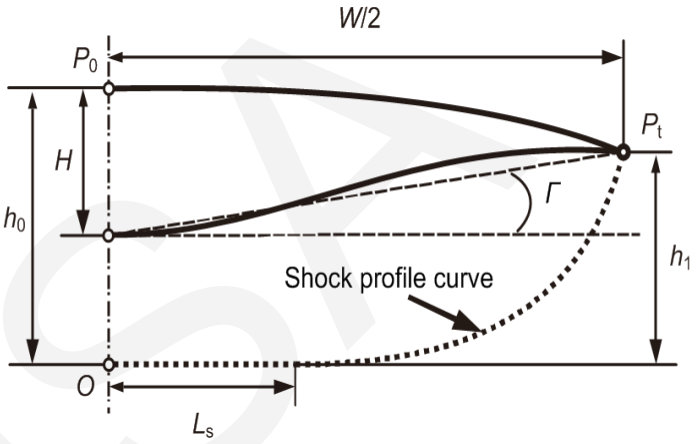


Fig. 9 Waverider geometric characteristics curves on base plane (right half)

As shown in Fig. 8, two constant sweep angles (Λ_1 and Λ_2) are applied to the waverider planform leading edge. The constraint of sweep angles between the aspect ratio is presented in Eq. (8). As shown in Fig. 9 , the dihedral angle Γ can be adjusted by the shock profile curve function based on its undetermined coefficient A as shown in Eq. (11) .

$$\min\left(\tan\Lambda_1, \tan\Lambda_2\right) < \tan\Lambda < \max\left(\tan\Lambda_1, \tan\Lambda_2\right). \quad (8)$$

$$A = \frac{h_1}{\left(\frac{W}{2} - L_s\right)^3} = \frac{L_W \tan\beta_s - H + \frac{W}{2}\tan\Gamma}{\left(\frac{W}{2} - L_s\right)^3}. \quad (11)$$

重要结果

1、The validation of design methodology of osculating cone waverider with adjustable sweep and dihedral angles.

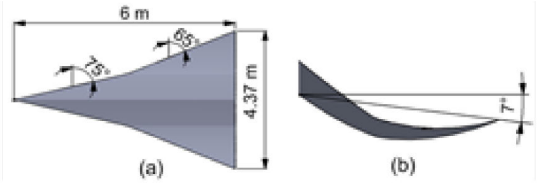


Fig. 11 Shape views and geometrical parameters of Case 1 (half model)
(a) Planform view; (b) Rear view

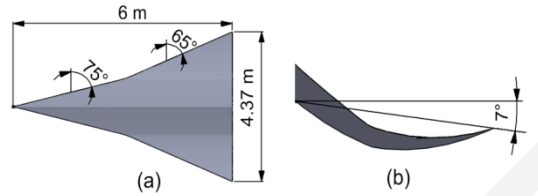


Fig. 12 Shape views and geometrical parameters of Case 2 (half model)
(a) Planform view; (b) Rear view

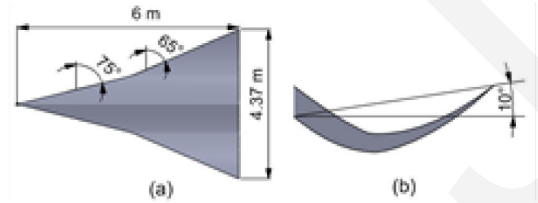


Fig. 13 Shape views and geometrical parameters of Case 3 (half model)
(a) Planform view; (b) Rear view

- The verification cases.

The planform and rear view of Cases 1–3 are illustrated in Figs. 11–13, respectively. As shown in Figs. 11a and 11b, the leading-edge sweep angles of Case 1 are Λ_1=75° and Λ_2=65° , and the dihedral angle (Γ) of Case 1 is set as −7° which is also defined as the positive anhedral angle.

- The validation of design methodology by numerical simulation.

As illustrated in Fig. 14, the predicted shock wave location obtained by the numerical method matches well with the designed shock wave profile curve denoted as the dashed curve.

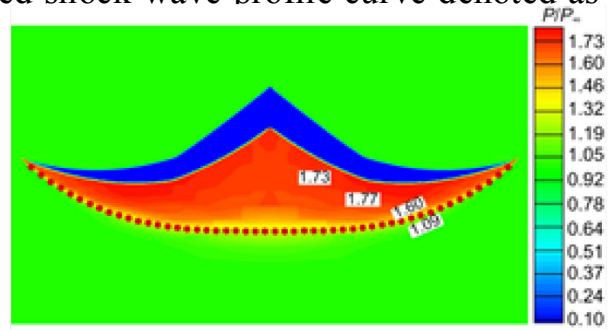


Fig. 14 Dimensionless pressure contour of Case 1 on the base plane

重要结果

1、The influence evaluations of dihedral and sweep angle on the lateral stability and lift-to-drag ratio of waverider.

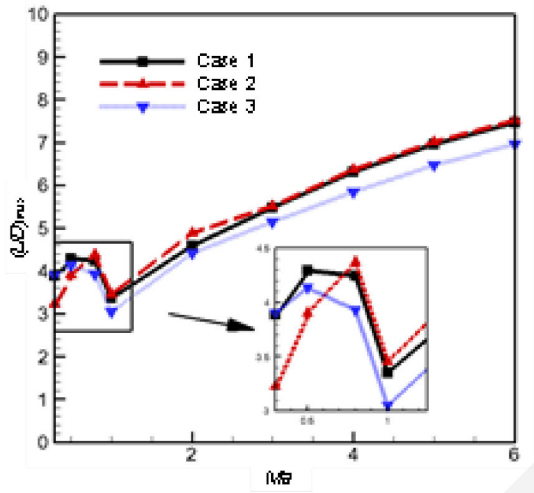


Fig. 19 Curves of maximum lift-to-drag ratio over Mach numbers of Cases 1–3

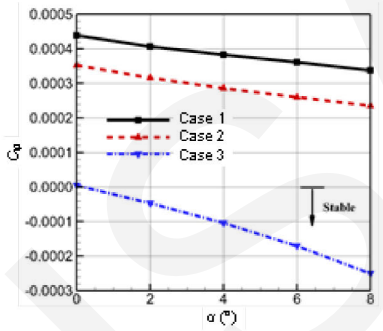


Fig. 21 Curves of lateral stability derivstive over attack angles of Cases 1–3 (Ma=6.0, β=0°)

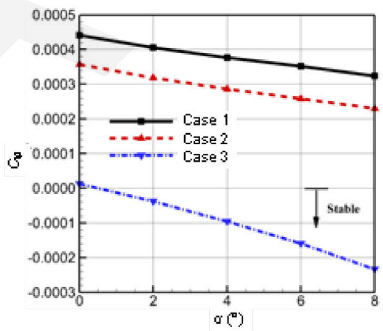


Fig. 22 Curves of lateral stability derivative over attack angles of Cases 1–3 (Ma=6.0, β=2°)

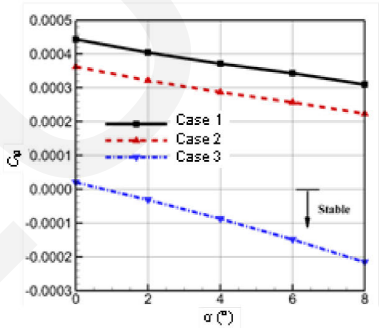


Fig. 23 Curves of lateral stability derivstive over attack angles of Cases 1–3 (Ma=6.0, β=3°)

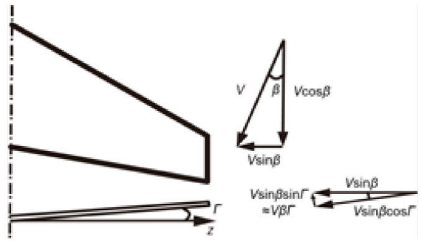


Fig. 24 Effective attack angle change caused by sideslip angle β

结论

■ **Regarding the maximum lift-to-drag ratio：**

- **The sweep angle plays a role on the lift-to-drag ratio only at subsonic and trans/supersonic speeds as a negligible effect is observed at hypersonic speeds, whereas the dihedral angle is seem to produce a relevant difference at hypersonic speeds.**
- **The effect of sweep angle on maximum lift-to-drag ratio is contradictory at subsonic and trans/supersonic speeds. At the subsonic speed flight stage, the parameter Λ_1 produces higher efficiency at smaller angles. For waverider design,**

■ **Regarding the lateral static stability of a waverider:**

- **The dihedral angle is more important to the lateral stability of a waverider than the sweep angle.**
- **The results show that the dihedral angle is beneficial for lateral stability.**

JZUSA